

ACOUSTIC EMISSION AS A FRICTION FORCE INDICATOR AFTER TEST STANDS EXPERIMENTS

Burhard Ziegler

University of Applied Sciences
35390 Giessen, Wiesenstraße 14
tel.: +49 641 3092226, fax: +49 641 3092911
e-mail: Burkhard.Ziegler@mmew.fh-giessen.de

A. Miszczak

Gdynia Maritime University
Morska 83, 81-225 Gdynia, Poland
tel.: +48 58 6901348, fax: +48 58 6901399
e-mail: miszczak@am.gdynia.pl

Abstract

This paper describes the use of acoustic emission measurement as an indicator of friction force into hydrodynamic journal bearings. The parameters load, speed, friction force, oil-temperature as well as the displacement of the sleeve are mainly measured in mutual dependence in journal plain bearing test stands. The friction force can not be measured directly, it must be calculated from the reaction force of the sleeve. Many different constructions are in use with the aim to load the bearing with a minimized influence of friction force measurement. Because of the huge influence to the friction force it is desirable to have parameters that are corresponding with it and are independent of the bearing load. We investigate the applicability of the acoustic emission analysis to indicate the friction force at an existing plain bearing test stand. The adoption of the acoustic emission measurement system (the diversion of the waves from the sleeve, the wave propagation through the AE transducer, the measurement chain and the damping of the mechanical and electrical disturbance) onto the test stand is described.

Keywords: non-destructive testing, acoustic emission, plain bearing, friction force

Zusammenfassung

Dieser Artikel beschreibt den Einsatz der Schallemissionsanalyse als Indikator der Lagerreibung in hydrodynamischen Gleitlagern. In Gleitlagerprüfständen werden hauptsächlich die Parameter Last, Drehzahl, Reibkraft, Öltemperatur sowie die Verlagerung der Lagerschale in gegenseitiger Abhängigkeit gemessen. Da sich die Reibkraft nicht direkt messen lässt, wird sie durch die Reaktionskraft der Lagerbuchse bestimmt. Zur Lasteinleitung sind verschiedene Konstruktionen bekannt, die alle darauf zielen, die Beeinflussung der Reibkraftmessung durch die Einleitung der Last zu minimieren. Wegen des großen Einflusses der Reibkraft auf die Beurteilung des Reibungszustandes in Gleitlagern ist es wünschenswert, einen von der Lasteinleitung unabhängigen Messwert zu haben. So wird untersucht, inwieweit die Schallemissionsanalyse an einem vorhandenen Gleitlagerprüfstand die Reibkraft abbildet. Die Adaptation des Schallemissionsmesssystems (die Ableitung der SE-Wellen aus der Lagerbuchse, die Weiterleitung an den SE-Sensor, die Messkette sowie die Erkennung und Eindämmung der mechanischen und elektrischen Störgrößen) an dem Prüfstand sowie die erfolgten Untersuchungen werden beschrieben. Zum Abschluss erfolgt eine Bewertung der Ergebnisse.

Schlüsselwörter: zerstörungsfreie Werkstoffprüfung, Schallemissionsanalyse, Gleitlager, Lagerreibung

1. Preliminaries

This paper describes the use of acoustic emission measurement as an indicator of friction force into hydrodynamic journal bearings. The investigation was carried out at the plane bearing test stand of the Maritime University Gdynia (Poland) Faculty mechanical engineering. The University of Applied Sciences Giessen-Friedberg (Germany) places the acoustic emission equipment at

bilateral disposal. This cooperation is based on the TOK-FP6, MTKD-CT-2004-517228, Biobearing. The adoption of the acoustic emission measurement system onto the test stand, the experiments and the results are described.

2. Short introduction into Acoustic Emission

Acoustic Emission (AE) is defined in general as transient elastic waves generated from rapid release of strain energy caused by deformation or damage within or on the surface of material [9]. AE differs from ultrasonic testing, which actively probes the structure; AE listens for emissions from active defects and is very sensitive to defect activity when (e.g. in a proof test) a structure is loaded beyond its service load [3]. During detecting and analysing the generated acoustic emission we earn information about the behaviour, state or quality of these acoustic emission sources. The frequency domain of the elastic waves emitted by the sources extends from the infrasonic up to the ultrasonic frequency area. Earthquakes generate acoustic emission waves in the infrasonic frequency area. The frequency of the so called cry of tin lies in the human acoustic range. Liquid friction, boundary friction and breaking processes generate acoustic emission in the ultrasonic area. The frequency domain of acoustic emissions ranges between 30 kHz and 2 MHz generally. By limitation of the lower frequencies, low-frequency interferences are removed. For physical reasons the amplitude of the oscillations drops strongly with an increasing frequency. The aforementioned frequency domain therefore represents an optimum, because the signal-to-noise ratio has there its maximum. To detect AE it is necessary to have an AE-transducer, who transforms the elastic waves into an electrical signal. Nowadays piezoelectric transducers are state of the art. In these transducers a piezoelectric disk transforms the incoming mechanical wave into a corresponding electrical signal. Every transducer has its own characteristic e.g. resonate- or wideband-transducer. The earned electrical signal must be amplified and filtered and then it can be registered or computed. There are a couple of identification values and methods to characterise an AE source with the measured AE-signal (rise-time, fall-time, peak-to-peak-value, duration, energy, Root-Mean-Square-Value, Cross-Correlation, Fast-Fourier-Transformation, Wavelett-Transformation a.s.f.) [3, 6, 9].

3. The generating of Acoustic Emission by fluid friction

The fluid friction between the oil-layers inside the clearance of the investigated hydrodynamic journal bearing is the energy source to generate the elastic waves. In hydrodynamic journal bearings a shaft rotates eccentrically in a sleeve. The pump action of the rotating shaft delivers the lubricant into the bearing clearance and with convergent bearing clearance brings about the build-up of oil pressure [4]. This oil pressure separates the sliding surfaces from each other. The oil adheres in thin layers to the sleeve surface and on the other side of the clearance at the shaft surface. The thickness of these so-called boundary layers ($h_{B,SH}$ - thickness of the shaft boundary layer; $h_{B,SL}$ - thickness of the sleeve boundary layer) depends on the roughnesses of the surfaces. The shaft rotates with $\omega > 0$ the sleeve stands $\omega = 0$, so we have a speed gradient between this two surfaces in the oil. The velocity ($u = 2\pi \cdot n \cdot r$) increases from the outer to the inner radius (r) of the clearance. That means there are different oil-layers with different velocities existing in the bearing clearance. The higher the speed difference between two layers the faster the oil molecules bumping against their neighbours as they are passing. As the layers pass each other, on average the molecules in the faster stream are slowed down, and those in the slower stream are speeded up. The smaller the lubrication gap (h) the more often the bumpings of the oil molecules. Therefore the kinetic energy of the layer is transformed into heat energy [8]. This connection is describes by the shear rate ($D = u / h_{eff}$). The difference of the gap height (h) and the two boundary layers is the effective gap height ($h_{eff} = h - h_{B,SH} - h_{B,SL}$). The shearing volume increases with the width of the lubrication gap therefore the transformed energy also increases. The generated heat also increases according to the dynamic viscosity (η). Besides that shear stress ($\tau = \eta \cdot D$) exists between the oil-

layers. Parts of the energy are conducted as elastic fluid-waves through the clearance of the journal bearing. At the interface of the sleeve the fluid-waves are transformed into mechanical waves which propagate into the sleeve material.

4. Description of the original test stand

The shaft (Brass MO58) of the used journal bearing test stand has a diameter of 99.93 mm and is powered by an electric engine, which itself is driven by a frequency drive (Hitachi SJ 100). The number of revolutions can be changed by this frequency drive. The frequency drive controls the engine resolution by itself at a constant value. The used sleeve (PCM100105115B SKF) has an inside diameter of 100.21 mm and a width of 80 mm and is moulded in a 7 mm thick aluminium guide bushing. These are fixed in a strain frame. The bearing-load can be increased or decreased by changing the weights at the strain frame. These changes have an effect directly onto the sleeve. The horizontal and the vertical displacements of the sleeve during the test are measured by special sensors (Megatron MDCT 2-K-2410). The friction force can not be measured directly but has to be calculated by the measured reaction force of the sleeve, considering the lever-arms. The reaction force is measured by a force-sensor (Megatron KT 1400 K 200). The bearing back temperature and the oil temperature are measured by Pt 100 sensors. All described sensors are connected with a multi-channel measurement device (UPM 100, Fa. Hottinger-Baldwin). The lubricating oil will be pumped from the oil reservoir with a heater/cooler combination into the bearing clearance through the oil inlet at the bottom side of the sleeve. The oil pressure has to be regulated with by valve by hand. "LOTOS Mineralny SAE 15W40" motor oil has been used for this investigation.

5. Description of the adapted test stand

To transducer the generated mechanical waves into electrical signals we need an Acoustic Emission transducer (AE-transducer). This transducer can not be placed directly on the sleeve, because it could be damaged by the temperatures, which are existing in the test stand. Therefore we have to transmit the mechanical waves from the sleeve by a waveguide outside the test stand casing. The waveguide is specially constructed for this investigation, it consists of three parts: the sleeve-adapter, the rod and the sensor-adapter. The sleeve-adapter has the same shape on its bottom side like the sleeve on its outside and is fixed with a heat-resistant glue on it. The geometry and the lack of any parallel surfaces reduce the number of mechanical resonances in the sleeve-adapter. Therefore he conducts - with low damping- the mechanical waves out of the sleeve directly into the rod. The rod conducts the mechanical waves out of the test stand to the conic adapter and the sensor. All passages in between the waveguide are constructed smoothly to protect interferences and damping. The AE-transducer (Piezo Test 0,15 ESS 20), which is placed at the sensor-adapter, transforms the mechanical waves into corresponding electrical signals. They both are coupled by a high viscosity grease to permit the transmission of mechanical waves. The electrical signals are conditioned by an amplifier and a band pass-filter (PAC 1220 Preamplifier) to intensify the signals as well as to reject the environmental, mechanical and electrical noises. Also for these protecting purposes, the transducer, the amplifier and the Root-Mean-Square-device (AD 536A) [8] are surrounded by a sheet metal housing. To reject electrical noises that are occurring from the power line, the power supply of the amplifier as well as the RMS – module is ensured by a power pack which has a special filter unit. The outgoing signals are spitted parallel to the first channel of a digital oscilloscope (Tektronix TDS 210) as well as to a RMS-device. After passing the RMS-device, the signals go through the second channel of the oscilloscope. The oscilloscope is connected to a computer via interface for data achievement and controlling purposes. The computer is also connected to an UPM 100 to collect temperature, force and displacement value details. The UPM 100 and the oscilloscope unit are driven by an especially developed program (written in DELPHI 7®). The block diagram of the used measurement chain is shown in Fig.2.

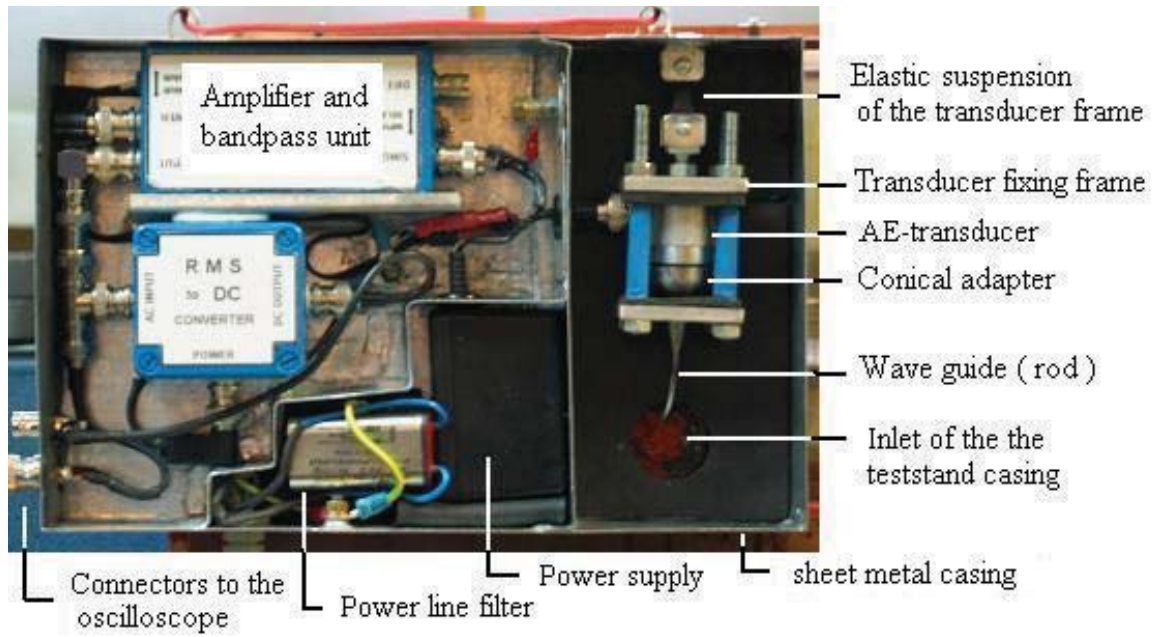


Fig. 1. The acoustic emission devices into the sheet metal casing (without cover)

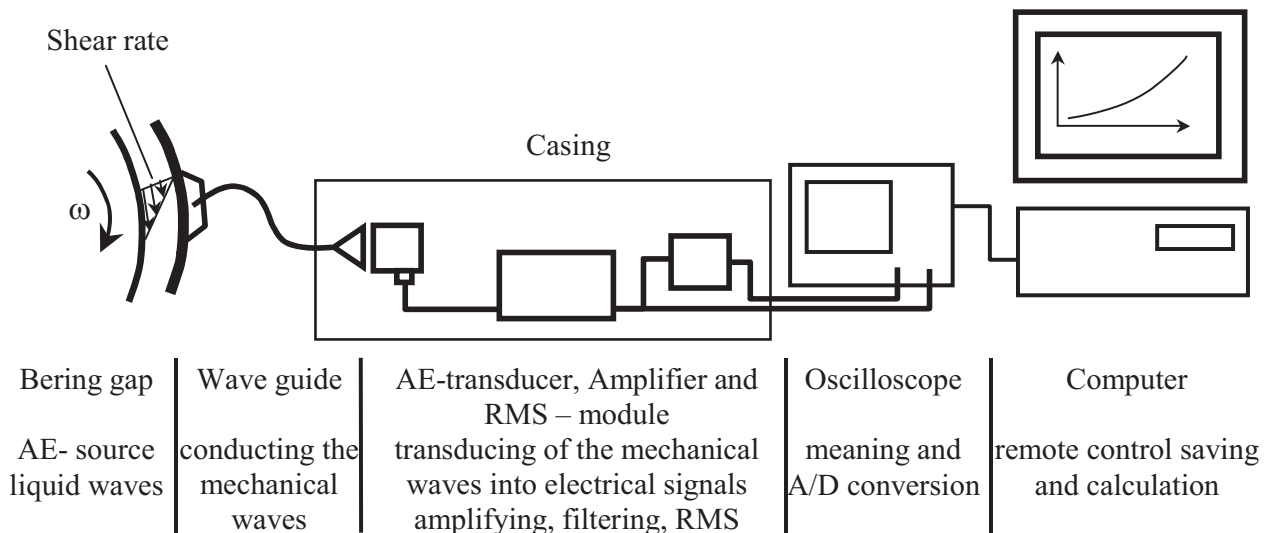


Fig. 2. Block diagram of the used measurement chain

6. Course of the experiments

First the oil was heated up to its operating temperature and then pumped into the test stand. By turning the shaft below small load and low speed all parts of the test stand achieved her operating temperature. We followed the course scheme shown in Fig. 3, so we got data for 3 different shaft speeds and for every shaft speed 8 different bearing loads. The measuring of the dates started with a high shaft speed and a less load. Step by step the load was increased (from 216N to 1785N) and the measurements for each load up to the maximum load were repeated. Each test had a constant shaft speed. Then the shaft speed was decreased and the procedure was repeated. At the beginning of each measurement the bearing back temperature had to be 80 ± 1 °C and the lubrication oil temperature had to be 69 ± 1 °C. At each step of the experiment we measured all values synchronically by the oscilloscope as well as the UPM 100, both controlled by the specially developed program.

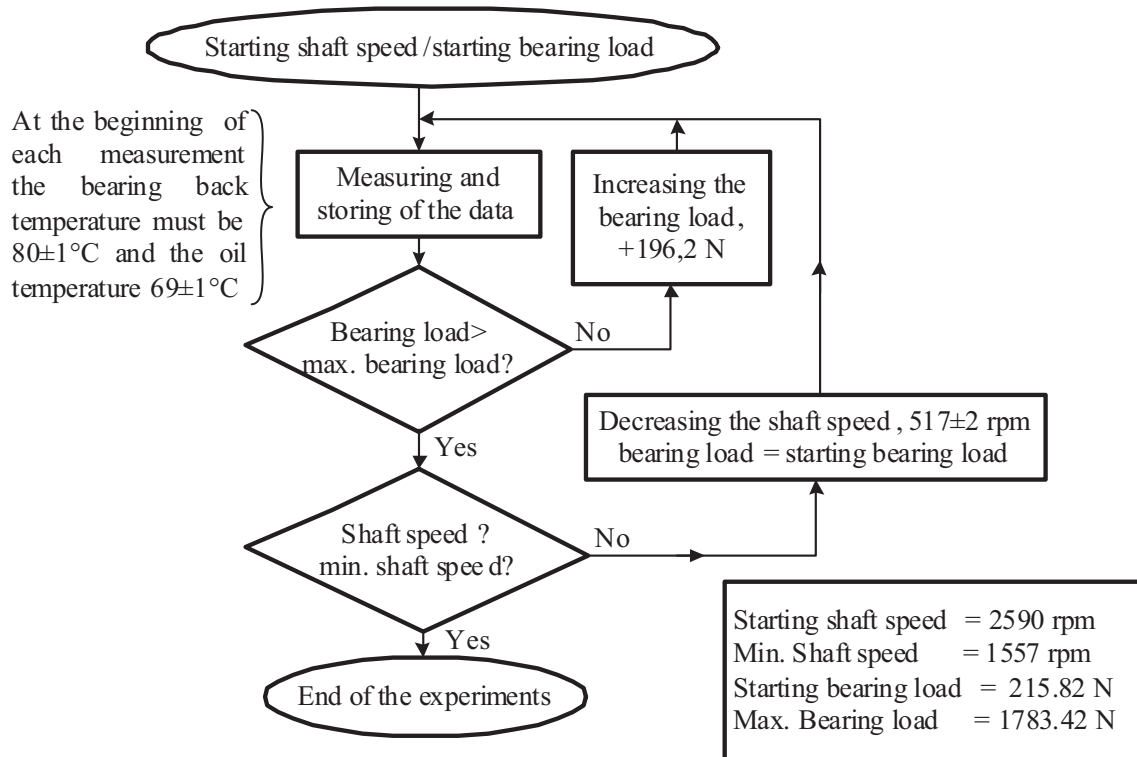


Fig. 3. Shows the course scheme of the measurements. If we follow this scheme, we get data for 3 different shafts speed and for every speed 8 different bearing loads

7. Results of the experiments

Physically the RMS-value is a power quantity and the friction force is a work quantity. To compare these quantities we must convert the friction force into friction power. Therefore we multiply the single friction force values with the lever arm and the angular velocity of the respective series of measurement. We entered the measured RMS-values and the calculated Friction Power values into diagrams {(Friction Power [W], RMS [mV]) vs. speed [min^{-1}]}. Fig. 4a, Fig. 4b, Fig. 4c and connect them with straight lines (Excel®).

The Friction Power values increase nearly linear according to bearing load. The values regarding different shaft speeds rise according to the increasing of the speed. The RMS-value is also increasing regarding to the bearing load and according to the shaft speed. The RMS-values have partially a higher spread than the Friction Power values. The higher the rotational speed, the larger the spread of the values. The diagrams show a great similarity between the RMS-values and the Friction Power values regarding increasing bearing loads and the changing of the shaft speed.

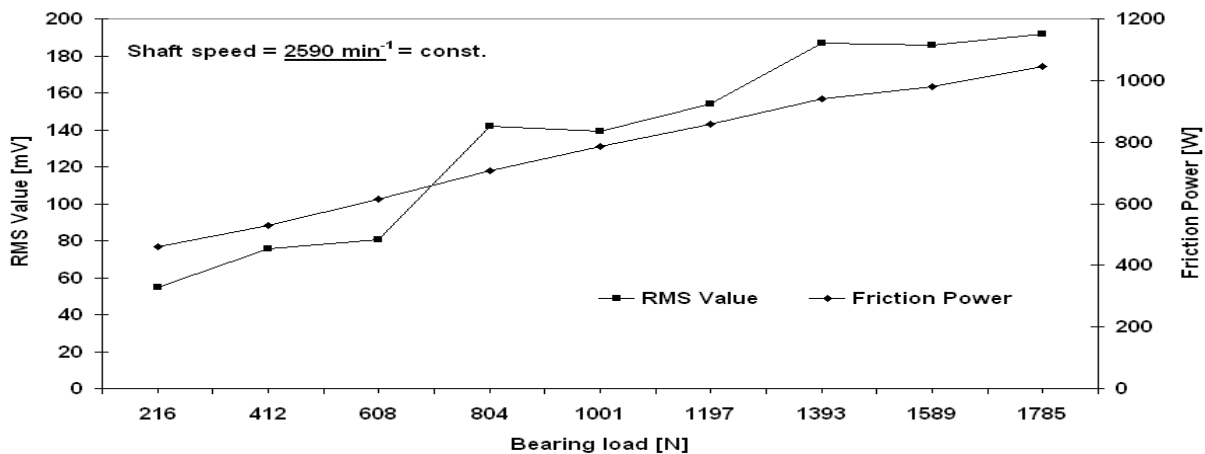


Fig. 4a. Comparison between the RMS-value and the calculated Friction Power at a shaft speed of 2590 rpm and bearing loads from 216 N up to 1785 N

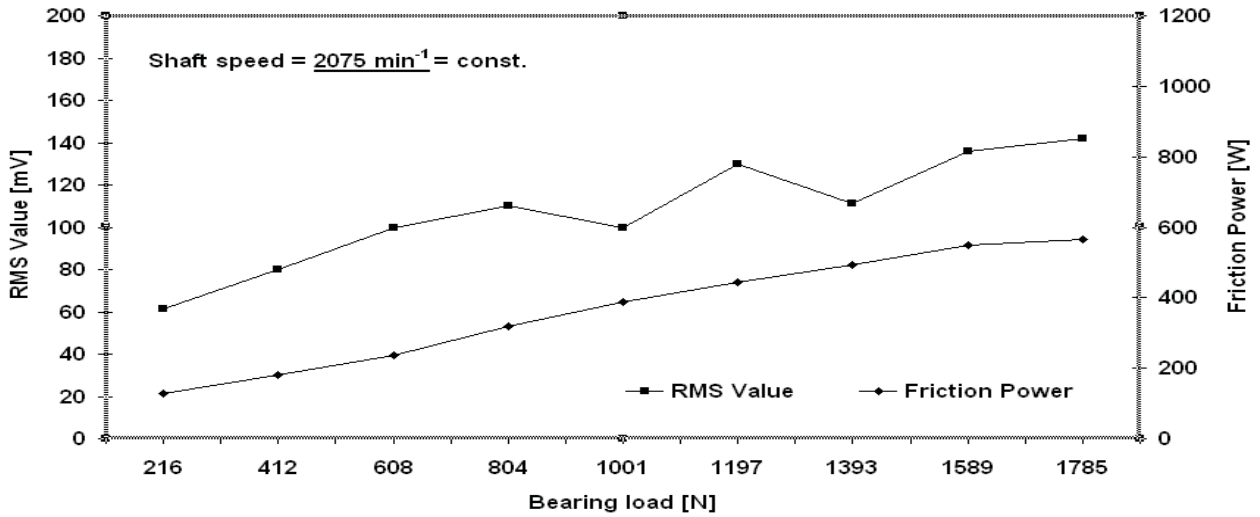


Fig. 4b. Comparison between the RMS-value and the calculated Friction Power at a shaft speed of 2075 rpm and bearing loads from 216 N up to 1785 N

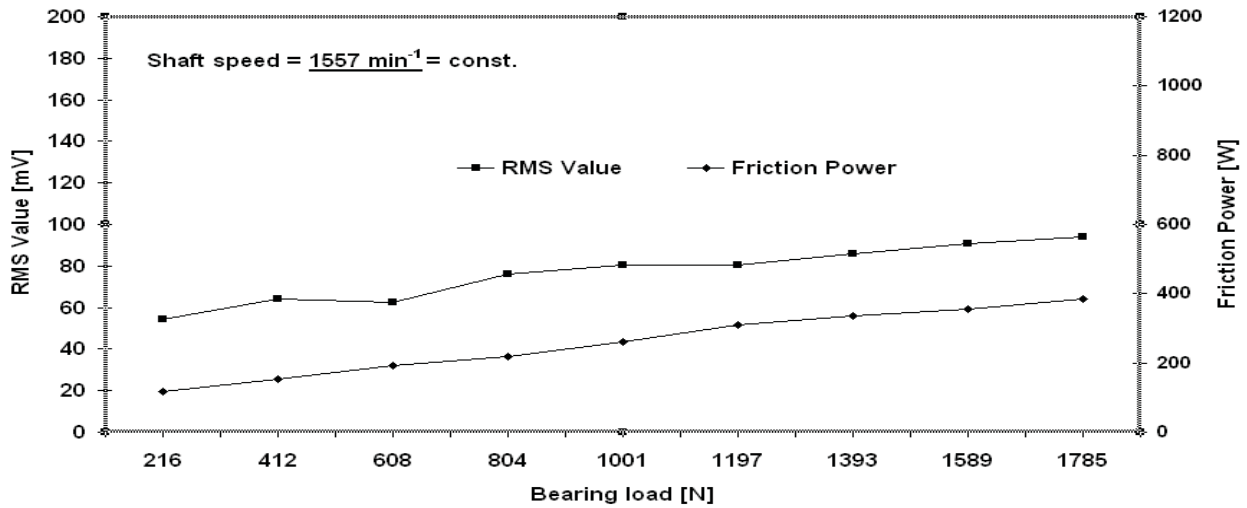


Fig. 4c. Comparison between the RMS-value and the calculated Friction Power at a shaft speed of 1557 rpm and bearing loads from 216 N up to 1785 N

To compare the RMS-values of the different shaft speed series, a characteristic number is necessary, which represents the different hydrodynamic burden conditions of the bearing. The Sommerfeld number represents these conditions [2, 4, 7]. The Sommerfeld number is defined:

$$So = (p \cdot \psi^2) / (\eta \cdot \omega), \quad (1)$$

where:

- p - mean surface pressure [Pa],
- ψ - relative bearing play [-],
- η - dynamic viscosity [Pas],
- ω - angular velocity [s⁻¹].

In our case the exact dynamic viscosity of the lubrication oil is unknown, because the dynamic viscosity depends on the temperature inside the bearing clearance. The measured bearing back temperature represents the oil temperature not exactly. To get independent of (η), both pages of the equation (1) are multiplied by factor (η). Fig. 5a shows the RMS-values and Fig. 5b the Friction Power values from the three series of measurement at different bearing burden condition versus the ($So \cdot \eta$) numbers. These diagrams are also showing the great similarity between the RMS-values

and the Friction Power values. As shown in Fig. 5a the spread of the RMS-values depends on the angular velocity, which corresponds with the shaft speed.

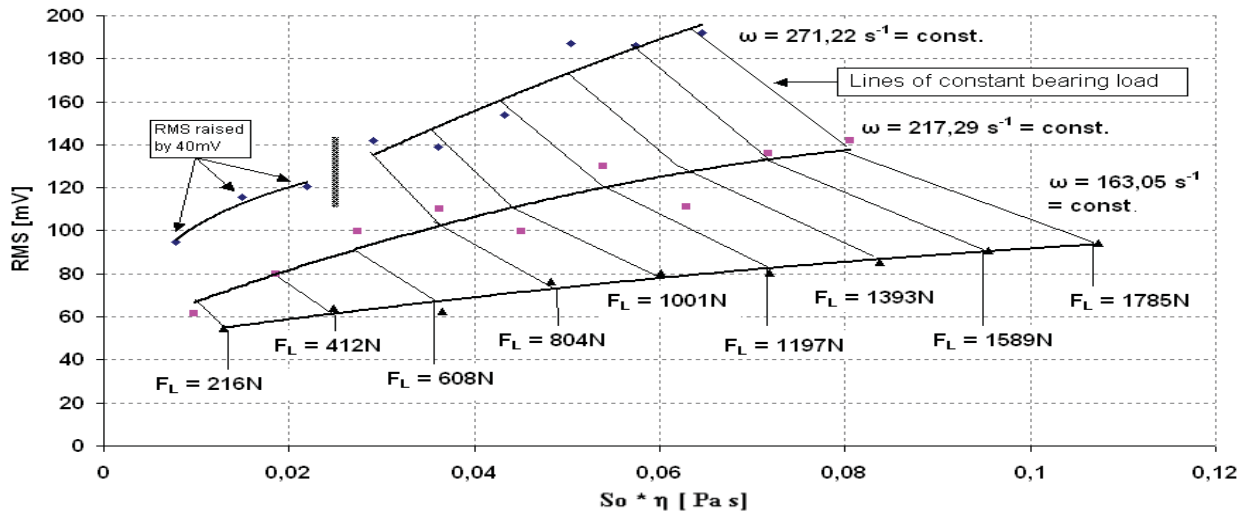


Fig. 5a. RMS-values of different series of measurement versus the extended Sommerfeld number ($So \cdot \eta$)

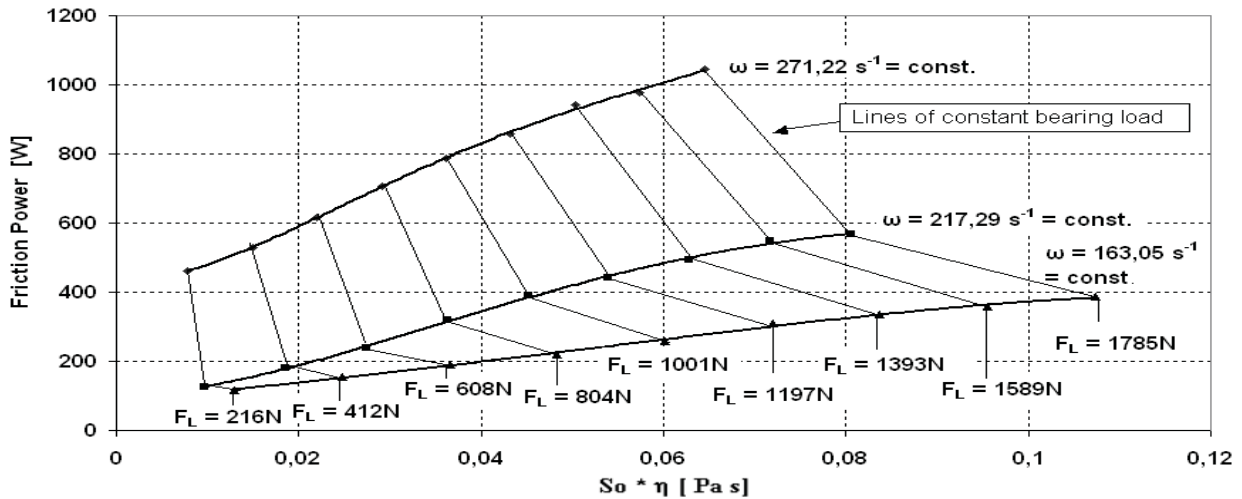


Fig. 5b. Friction Power values of different series of measurement versus the extended Sommerfeld number ($So \cdot \eta$)

The Sommerfeld number tells us that a high angular velocity in combination with a low bearing load leads to a low bearing burden. Low burden can lead to oscillations of the shaft which's changes the bearing gap. The change of the bearing gap height (h_{eff}) causes changes of the shear rate (D) and thus also generates different Acoustic Emission intensities. In Fig. 5a the series of measurement with an angular velocity of 271.22 s^{-1} show a discontinuity at the first three RMS-values at low bearing load which results from the low bearing burden in combination with the high shaft speed. The Friction Force values in the Fig. 5b show a steady-going run of the curve which can be explained by the inertness of the measuring method and influences occurring by the weight installation.

8. Conclusions

The investigations have shown that the acoustic emission analysis is suitable as indicator of the bearing friction at journal plain bearings. The results show a great similarity between the RMS-values and the Friction Power values regarding increasing bearing loads and the changing of the shaft speed. The measured values point out that the Acoustic Emission Analysis reacts to the

modification of the friction conditions inside of the bearing faster than the Friction Force values. The RMS-values are related to the geometry of the bearing and the acoustic emission measuring chain. The measured RMS-value of the acoustic emission is a qualitative value of the friction conditions in journal plain bearings. For these reason one can not assign the RMS-values to other journal slide bearing directly. Every bearing has its one condition, which have to be considered (wave propagation, wave damping, and transmission of the mechanical waves from the sleeve by a waveguide to the AE-transducer).

Acknowledgement

We would like to thank Prof. Dr. habil. K. Wierzcholski (Gdynia Maritime University, Gdynia, Poland) and Prof. Dr. Ing. H.-J. Schwalbe (University of Applied Science, Gießen, Germany) very cordially. At any time they supported us technically and organizationally at the leading-in conductor as well as the assessment of the experiments.

The present research is financially supported within the frame of the TOK–FP6, MTKD-CT-2004-517226.

References

- [1] ASTM E 976-94, *Standart Guide for Determining the Reproducibility of Acoustic Emission Sensor Response*, American Society for Testing and Materials, Philadelphia, USA.
- [2] Czichos, H., Habig, K. H., *Tribologie - Handbuch Reibung und Verschleiß*, Auflage 2003, Vieweg & Sohn Verlag, Wiesbaden.
- [3] Eisenblätter, B, Schwalbe, H. J., et al., *Einführung in die Schallemissionsanalyse*, Battelle Institut, Ffm.
- [4] Grothe, K. H., Feldhusen, J., *DUBBEL Taschenbuch für den Maschinenbau*, Auflage 2005, Springer, Berlin Heidelberg New York.
- [5] <http://galileo.phys.virginia.edu/classes/152.mfl1.spring02/Viscosity.pdf>.
- [6] Krautkrämer, J., Krautkrämer, H., *Ultrasonic Testing of Materials*, Translation of the 5th Revised German Edition, Auflage 1990, Springer, Berlin, Heidelberg.
- [7] Muhs, D., Wittel, H, Jannasch, D., Voßiek, J., *Roloff / Matek Maschinenelemente*, Auflage 2005, Vieweg & Sohn Verlag, Wiesbaden.
- [8] www.analog.com/en/prod/0%2C2877%2CAD536A%2C00.html.
- [9] www.ndt.net/ *Non-destructive Testing Encyclopedia*.